

# Strong Correlation between Molecular Configurations and Charge-Transfer Processes Probed at the Single-Molecule Level by Surface-Enhanced Raman Scattering

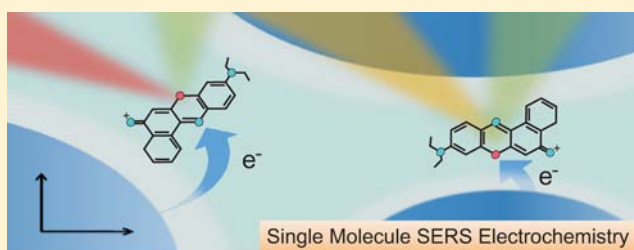
Emiliano Cortés,<sup>\*,†</sup> Pablo G. Etchegoin,<sup>‡</sup> Eric C. Le Ru,<sup>‡</sup> Alejandro Fainstein,<sup>\*,§</sup> María E. Vela,<sup>†</sup> and Roberto C. Salvarezza<sup>†</sup>

<sup>†</sup>Instituto de Investigaciones Físicoquímicas Teóricas y Aplicadas (INIFTA), Universidad Nacional de La Plata-CONICET, Sucursal 4 Casilla de Correo 16 (1900), La Plata, Argentina

<sup>‡</sup>The MacDiarmid Institute for Advanced Materials and Nanotechnology, School of Chemical and Physical Sciences, Victoria University of Wellington, PO Box 600, Wellington, New Zealand

<sup>§</sup>Centro Atómico Bariloche and Instituto Balseiro, Comisión Nacional de Energía Atómica and Universidad Nacional de Cuyo, (8400) San Carlos de Bariloche, Río Negro, Argentina

**ABSTRACT:** Single-molecule (SM) electrochemistry studied by surface-enhanced Raman scattering (SERS) with high spectral resolution reveals a picture in which the frequency of Raman modes is correlated with the electrochemical process through the interaction with the surface. Previously unexplored phenomena can be revealed by the synergy of electrochemistry and SM-SERS, which explores in this case subtler spectroscopic aspects (like the frequency of a vibration within the inhomogeneous broadening of a many-molecules Raman peak) to gain the information. We demonstrate, among other things, that the interaction with the surface is correlated both with the molecule vibrational frequencies and with the ability of single molecules to be reduced/oxidized at different potentials along the electrochemical cycle. Qualitative models of the interaction of molecules with surfaces are also touched upon.



## I. INTRODUCTION

The possibility to monitor single-molecule (SM) redox processes with a variety of techniques<sup>1–3</sup> (optical or otherwise<sup>4–7</sup>) has always been a long-desired ambition in the field of electrochemistry.<sup>1–3,8–11</sup> Recently,<sup>12</sup> we have succeeded in demonstrating SM-electrochemistry monitored with a specific optical technique with high vibrational specificity, surface-enhanced Raman scattering (SERS).<sup>13,14</sup> This current work builds up on that demonstration, by exploiting a higher time resolution of the electrochemical cycle on a new CCD detector, as well as subtler aspects of the spectroscopic signatures of SM-SERS (like the existence of inhomogeneous broadenings in Raman peaks<sup>15</sup>). We shall aim at establishing a link between the redox potentials of different single molecules and the line spectral position within the inhomogeneous broadening of a particular Raman peak of the analyte. This link, it is argued, reveals the different interactions of single molecules with the surface, which affects simultaneously the spectroscopic Raman features and the redox potentials. In that manner, it reveals a much subtler aspect of the electrochemistry of SM's than those observed before,<sup>12</sup> which were merely aimed at demonstrating the possibility of SM-SERS electrochemistry.

For our purposes here, all of the aspects related to the actual detection of SM's in SERS rely very heavily on the accumulated experience of the last 5–10 years, which reveals in its full details

how to actually carry out these experiments. This information has been extensively reviewed in the literature over the past few years,<sup>13,16–23</sup> and we shall only repeat here key elements for convenience and ease of presentation. A recent review article covering essential aspects of SM-SERS, and (in particular) the bialyte method used in the present experiments, can be found in ref 24 for the interested reader.

## II. EXPERIMENTAL DETAILS

**A. Experimental Setup.** A three-electrode cell with a Ag/AgCl (1 M Cl<sup>-</sup>) electrode and a high-area platinum foil as reference and counter electrodes, respectively, was used. The working electrode was immersed in the electrolyte solution (phosphate buffer, pH = 6), and this was placed inside an open electrochemical cell that allowed focusing on the substrate with long working distance objectives (×10, ×20, ×50, or ×100) through a water/air interface. All of the potentials reported here were referenced to a Ag/AgCl (1 M Cl<sup>-</sup>) electrode. Cyclic voltammetry was performed with a potentiostat with digital data acquisition. For single-molecule experiments, a scan rate of  $v = 0.20$  V/s was used ( $v = 0.40$  V/s in the case of two successive cycles), and potentials were scanned from  $-0.50$  to  $-0.10$  V. As previously reported, there are two pH-dependent redox mechanisms ( $2e^-2H^+$  or  $2e^-1H^+$ ) for NB on Ag, with the threshold for the different behaviors

Received: December 14, 2012

Published: February 5, 2013

occurring at  $\text{pH} = 6.1$ .<sup>25</sup> Cotton et al. have also shown that in the low pH regime ( $\text{pH} < 6.1$ ), the SERS spectra of NB on Ag are very similar to the Raman spectra of NB in solution, and this has been associated to both NB molecules adsorbed with the aromatic plane oriented in a perpendicular fashion with respect to the Ag surface and a  $2e^-2H^+$  redox mechanism. On the other hand, in the high pH regime ( $\text{pH} > 6.1$ ), there is a strong modification of the Raman spectra between the adsorbed and the free NB molecules. This has been assigned to flat NB molecules adsorbed on Ag and a  $2e^-1H^+$  redox mechanism.<sup>25</sup> Under our experimental conditions ( $\text{pH} = 6$ ), both redox mechanisms could be operating simultaneously. However, we have verified that in our electrochemical cell, the SERS spectrum of adsorbed NB is practically the same as NB in solution,<sup>12,26</sup> indicating that the  $2e^-2H^+$  process is the main one, with both oxidized/reduced NB molecules representing cationic species.

The electrochemical cell was placed on top of a motorized  $x-y$  stage for microscopy (to allow exploration and mapping of the electrode) and was used in combination with a BX41 Olympus microscope attached to a Jobin-Yvon LabRam spectrometer. All of the experiments performed in this Article were done with the 633 nm line of a HeNe laser with 3 mW at the sample. Further details of the experimental setup can be found in ref 12. For samples with “high” concentrations of dyes (which for SERS standards is still only  $\sim 20\text{--}40$  nM), we are mainly interested in average signals on the substrate. Therefore, we typically use for these experiments the  $\times 10$  objective, to have a large spot diameter  $\sim 10$   $\mu\text{m}$ , and minimize photobleaching effects as much as possible. On the other hand, for single-molecule detection ( $\sim 5$  nM), the  $\times 100$  long-working distance objective and a high resolution 2400 lines/mm grating were used. The minimum acquisition time required to follow the dynamics of the electrochemistry is 100 ms (fixed by the total integration and processing times of the CCD). This integration time is well below typical photobleaching times for the present experimental conditions, and it allows the observation of single cycles, and sometimes two consecutive cycles, of SM-SERS events with many data points to follow the dynamics. We performed the corresponding blank experiments (voltammograms and spectra) under this experimental setup to test the system.

**B. Samples.** Nile Blue A (NB) and Rhodamine 6G (RH6G) were obtained from commercial sources (Sigma-Aldrich) and mixed at the appropriate concentrations with borohydride-reduced<sup>27</sup> Ag colloids (to avoid a citrate capping layer) and 20 mM KCl (to induce a slight destabilization and the formation of clusters<sup>28</sup>). For each specific case, details about the concentrations of the dyes used are described in the text. NB and RH6G adsorb to the colloids through electrostatic interactions. The colloidal solution is subsequently drop-casted and dried under a mild heat on a clean Ag foil electrode. Once dried, the colloids stick to the Ag foil by van der Waals forces, and remain attached to it upon reimmersion in the phosphate buffer solution. Several regions with multiple dried clusters of colloids can be easily distinguished in the microscope image on the Ag surface after drying. The Ag foil with the colloids and the dyes is our working electrode, and also provides the ideal means whereupon SERS enhancements produced by localized hot-spots (gap-plasmon resonances) can coexist with the ability to perform electrochemistry on the attached molecules. We checked at much higher concentrations ( $\sim 1$  mM) that, as far the voltamperogram is concerned, the electrochemistry of the dyes on the colloids is indistinguishable from the one where the dyes are directly attached to the Ag foil itself. Note also that in all of the experiments performed in this work the dyes were adsorbed previously on the colloids (i.e., the dyes are not dissolved in the electrolyte solution).

### III. EXPERIMENTAL RESULTS

**A. Many Molecules.** Figure 1 already summarizes a big fraction of the phenomenology we want to concentrate on, initially for the case of many molecules. In Figure 1a we show the electrochemical cycle obtained in the “many molecules” limit. We clearly label the oxidation (Ox) and reduction (Red) peaks in the cycle for NB on silver. By the same token, Figure

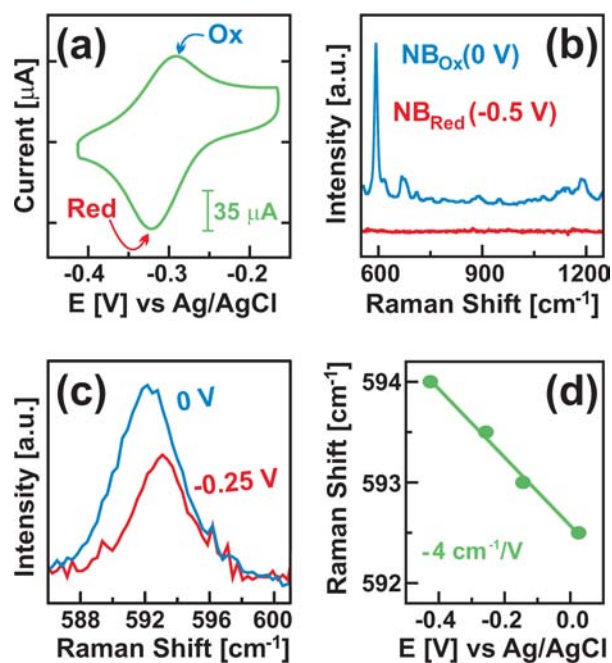


**Figure 1.** Many Nile Blue A (NB) molecules. (a) Cyclic voltammogram of NB adsorbed on Ag in phosphate buffer ( $\text{pH} \approx 6$ ) recorded at  $0.1 \text{ V s}^{-1}$ . Red/blue arrows show the peaks where NB molecules are reduced (red)/oxidized (ox), respectively. (b) Average SERS spectra at  $0/-0.5 \text{ V}$  of oxidized/reduced NB molecules, respectively (633 nm laser line, 3 mW,  $\times 10$  objective, 50 nM NB). The highly resonant oxidized state exhibits clearly the  $592.5 \text{ cm}^{-1}$  NB mode, whereas the nonresonant reduced NB has no SERS response in this spectral range. (c) The “fingerprint” region containing the  $592.5 \text{ cm}^{-1}$  mode of 50 nM NB at two different potentials:  $0 \text{ V}$  (blue) and  $-0.25 \text{ V}$  (red). There is a decrease in the intensity due to the reduction of a portion of the total amount of molecules and a blue-shift of the peak. (d) Linear dependence of the  $592.5 \text{ cm}^{-1}$  mode frequency of many NB molecules with the applied potential (slope:  $-4 \text{ cm}^{-1}/\text{V}$ ).

1b shows the average SERS spectra of many molecules in the oxidized and reduced states, respectively. The disappearing of the SERS spectra in the reduced state with respect to the oxidized one is due to a dramatic change in the resonance condition between the two, achieved by the charge-transfer process between the molecule and the metal. This is a well-known effect in the Raman electrochemistry of NB, and was already exploited by us in ref 12 to demonstrate single-molecule electrochemistry. Nevertheless, we aim now at adding an additional (arguably subtler) spectral information to the experiment. This is achieved by studying simultaneously the peak spectral position and shape of the strongest Raman fingerprint mode of NB at  $\sim 592.5 \text{ cm}^{-1}$ , while the electrochemical cycle is running in the background. On the basis of DFT calculations, this mode has been assigned to a collective ring-breathing mode of the structure. The basic result we will study at the single-molecule level is already visible (although with limitations to be explained later) in the many-molecule average spectra at two different applied potentials in Figure 1c. There, we take two SERS spectra while the sample is in the oxidized state ( $0 \text{ V}$ ) and while halfway-through to the reduced state ( $-0.25 \text{ V}$ ), as seen in Figure 1c. These spectra only concentrate on the fingerprint mode at  $\sim 592.5 \text{ cm}^{-1}$  with the high resolution grating (2400 lines/mm). It is clearly seen by eye that there is a systematic shift in the average frequency of the peak as a function of the applied potential. This is further

reinforced and summarized in Figure 1d, where we plot the average frequency of the peak for many molecules as a function of the applied potential ( $E$ ). This shift of the average peak position could be interpreted as a manifestation of a Stark effect affecting the molecules in the presence of the applied field.<sup>29</sup> A more careful analysis of the line width and shape, however, indicates that an alternative explanation could reside in a selective quenching of the Raman resonance for those molecules with smaller Raman shift within the inhomogeneous distribution of the many-molecule ensemble. We shall come back to the exact meaning of this later, but for the time being we are going to argue that this shift is indeed a manifestation of the fact that the interaction of the molecule with the substrate<sup>30–32</sup> changes both (i) the frequency of the mode within the inhomogeneous broadening of the peak (which is dependent on the proximity of the molecule to the surface),<sup>15</sup> and (ii) the electrochemical potential at which a specific molecule is reduced (which depends also on the proximity of molecule to the substrate, through the tunneling effect). Yet, first we need to establish the evidence for the effect at the single-molecule level. In doing so, we shall learn about the most likely scenario for the charge-transfer process of single molecules during the oxidation/reduction cycle, together with details that are washed out by the ensemble averaging nature of many-molecule signals. To this end, we need to establish first the conditions under which single-molecule spectra are observed. This is done in what follows.

Before that, it is important to note that the charge-transfer event that we mention in Figure 1 (and the rest of the text) is associated with an electrochemical redox reaction where two electrons and two protons are transferred from (to) the molecule to (from) the substrate. This is a completely different phenomenon from the traditional charge-transfer (CT) mechanism associated with the “chemical effect” in SERS.<sup>33</sup>

**B. Single Molecules.** The “single-molecule character” of a Raman spectrum can be decided by means of the bianalyte SERS technique, which has the ability to distinguish SM-SERS events in a statistical sense. In Figure 2, we review only very basic aspects of it for our purposes here, while leaving a more detailed analysis to the extensive list of papers and reviews published on the subject.<sup>13,16–23</sup> The method can be used with a bianalyte partner, which can be an isotopically edited version of the same molecule, or a different molecule altogether. It is preferable to use a bianalyte partner in our case here that does not respond to the electrochemical cycle in the range of potentials that are of interest for NB. This partner can be, for example, RH6G (as shown in Figure 2a). We have verified that the  $610\text{ cm}^{-1}$  mode remains unchanged during the electrochemical cycle, implying that RH6G is not affected in the potential window that we are using in our experiments. When looking at signals with a high resolution grating capable of distinguishing subtler details of the peak shapes, there is also an additional aspect to the problem. Single molecules can also be identified in this case by the presence of sharp signals within the inhomogeneous broadening of the peaks.<sup>15</sup> In fact, this has been already studied in quite some detail as an alternative to the bianalyte method itself in ref 15. Here, we can do both “discriminations” at the same time, and resolve single-molecule cases to add to the statistics. A few examples of single and many molecules cases (with different frequencies within the inhomogeneous broadening) are shown in Figure 2.

Once the validity for conditions of “single-molecule character” are identified, we can start eking through the

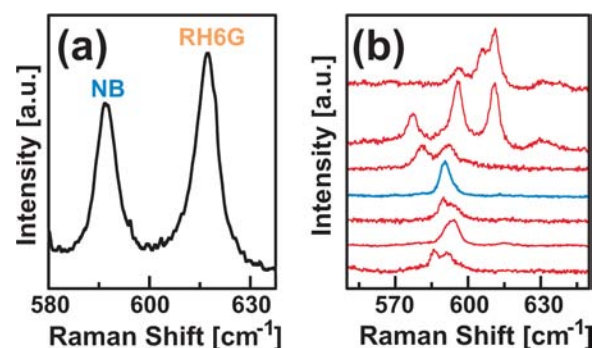


**Figure 2.** Bianalyte SERS method for single-molecule detection using Rhodamine 6G (RH6G) and Nile Blue A (NB). The “fingerprint” region containing the  $592.5\text{ cm}^{-1}$  (NB) and  $610\text{ cm}^{-1}$  (RH6G) modes was chosen to follow single-molecule events. (a) Average SERS spectra at open circuit potential over the sample after mapping more than 5000 points. (b) SERS spectra at different points of the sample at open circuit potential. Laser line  $633\text{ nm}$ ,  $3\text{ mW}$ ,  $\times 100$  objective, measured with a high resolution  $2400\text{ lines/mm}$  grating. Because of the high resolution, more than one molecule can be resolved simultaneously within the inhomogeneous broadening of the peak (either RH6G or NB).<sup>15</sup> Hence, more than two peaks can be found, that is, two NB peaks (in different “environments”) and one RH6G peak, or the opposite case. These cases (red spectra) are not considered as single-molecule events. Only those cases where a single (NB or RH6G) peak can be detected are considered as SERS single-molecule events (blue spectrum) for the statistics.

statistics to identify SM-SERS cases that satisfy them. Henceforth, we can establish a connection between the behavior for many molecules and that of SM-SERS signals in the light of the observed average softening of the frequency for the oxidized state seen in Figure 1c,d. A brief detour into specific SM-SERS cases is advantageous at this moment, and we do that in Figures 3 and 4.

Figure 3 shows the sudden appearance and disappearance of two single-molecule events (in the sense defined by the bianalyte method, vide supra), shown as both intensity (a,c) and Raman shift (b,d) evolution over the applied potential (or time). The intensity of the events turns out to be not correlated at all with the frequency of the Raman active vibration (an expected feature). Instead, the intensity of a given event is more related to the exact position that the molecule occupies with respect to the electromagnetic enhancement in the hot-spot.<sup>23,34</sup> The frequency, on the contrary, reports a much more fundamental physical parameter related to the interaction of the molecule with the surface.<sup>31,35</sup> We concentrate on the frequencies, with their main results being (i) the duration of the “on” state (oxidized) in independent SM-SERS events is different (within a range), revealing different oxidation/reduction potentials for different cases (a conclusion already reached in ref 12), and (ii) during the “on” state the Raman peak frequency of a single molecule remains constant within  $\pm 0.2\text{ cm}^{-1}$ . This is a repeatable feature of all of the SM-SERS cases we analyzed. As it stands, it suggests that the molecule remains “frozen” during the time where both electrons and protons are withdrawn (oxidation) in the configuration that is producing the interaction with the substrate. This interaction is revealed in the exact value of the frequency of the mode<sup>31</sup> within the inhomogeneous broadening of the peak.<sup>15</sup> The frequency is not dithering over that period, as it would be if the molecule was changing configurations on the surface. As such, these results also tell us something about the oxidation/



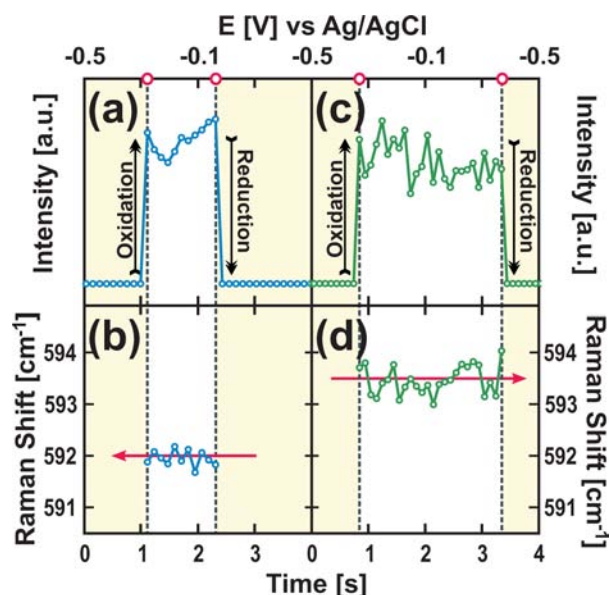


**Figure 3.** Monitoring single NB redox events through the high-resolution SERS signal in the “fingerprint” region containing the NB  $592.5\text{ cm}^{-1}$  mode. (a) SERS intensity profile of a single NB event obtained during a voltammetric run from  $-0.5$  to  $-0.1\text{ V}$  at  $0.2\text{ V s}^{-1}$  in our electrochemical cell. The “on/off” of the Raman signal corresponds to the oxidation/reduction potentials of that molecule:  $E_{\text{ox}} = -0.28\text{ V}$ ,  $E_{\text{red}} = -0.16\text{ V}$ . Integration time of the SERS signal  $t \approx 0.1\text{ s}$  per spectrum. (b) The Raman shift associated with the single NB event described in (a) is  $\sim 592\text{ cm}^{-1}$ . (c) SERS intensity profile of another single NB event:  $E_{\text{ox}} = -0.32\text{ V}$ ,  $E_{\text{red}} = -0.38\text{ V}$ . (d) The Raman shift associated with the single NB event described in (c) is  $\sim 593.5\text{ cm}^{-1}$ . Note that in (b) and (d) the values before/after the “jumps” are not shown as there is no NB peak in that regions (NB is reduced).

reduction process itself. Occam’s razor suggests that there is no evidence here for a “dynamic charge-transfer” scenario, even though if it was occurring at much faster frequencies we could arguably be seeing an average of it. The increased time resolution of these experiments with respect to previous ones<sup>12</sup> does provide a crucial upper limit of  $\sim 100\text{ ms}$  for that scenario. The simplest and most likely picture is that the molecule remains in its configuration during the oxidation cycle, and we speculate that the interaction of the “charged” molecule with its image, and with an anionic layer surrounding the NPs, during that time could be the main contributing factor for this stabilization. Most interestingly, we observe that SM-SERS events corresponding to one specific molecule are apparently allowed to relax to slightly different positions on the surface, either during the “off” (reduction) part of the cycle, or at the oxidation–reduction charge-transfer events (“jumps”). This is evidenced in Figure 4, for example, where single molecules could be followed in two consecutive electrochemical cycles (without photobleaching). What is seen in these circumstances is that the same signal can reappear with a different frequency from the first cycle. Whether such configuration changes happen during the “off” state of the molecule, following all of the standard stochastic perturbations that the molecule could experience at the surface, or when the charges (electrons and protons) are transferred to or from the molecule, is a central issue to which the SM-electrochemistry-SERS experiments, as we will demonstrate next, provide further insight. Once again, the increased time resolution of the experiment is crucial for the

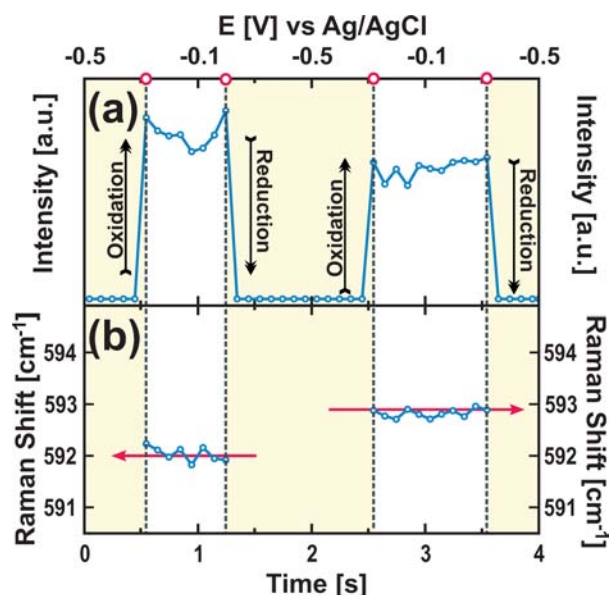


**Figure 4.** Two consecutive oxidation/reduction cycles of a single NB molecule shown again in (a) intensities and (b) frequencies. Not only do the oxidation/reduction potential points change from cycle to cycle for a particular molecule, but also the Raman frequency at which they appear. In the first cycle,  $E_{\text{ox}} = -0.26\text{ V}$ ,  $E_{\text{red}} = -0.22\text{ V}$ , and the Raman shift is  $\sim 592\text{ cm}^{-1}$ , while in the second one,  $E_{\text{ox}} = -0.26\text{ V}$ ,  $E_{\text{red}} = -0.30\text{ V}$ , and the Raman shift is  $\sim 593\text{ cm}^{-1}$ . There is evidence here that the molecule is allowed to “move” to a new configuration, either when it is in the reduced (silent) state, or during the two-electron and two-protons charge-transfer processes from and to the substrate (oxidation and reduction “jumps”). The slight change in intensity of the event can be linked to the same idea. Frequencies, however, remain locked-in at a given value within the resolution of the measurement in the oxidized state. The scan rate in this case is  $0.4\text{ V s}^{-1}$ .

observation of details like this one, that is, two consecutive electrochemical cycles before photobleaching takes place. Increased time resolution implies that successive electrochemical cycles can be run at a reasonable speed (to avoid photobleaching) without losing too much time resolution.

Figure 5 shows a completely new aspect of the problem that can only be observed with the ability to detect single-molecule electrochemical processes. As we demonstrated above, electrochemical potentials and Raman shifts fluctuate from molecule to molecule, and from cycle to cycle in one single molecule. On the contrary, a clear correlation exists between the reduction potential ( $E_{\text{red}}$ ) and the oxidized-state Raman shift for a specific SM-event (see Figure 5a). Indeed, molecules displaying larger Raman shifts are reduced at larger negative potentials. Also, correspondingly, molecules reduced at less negative potentials are characterized by smaller vibrational frequencies. Quite notably, as evidenced from Figure 5b, a similar correlation does not exist when we compare the observed (oxidized state) Raman shift and the potential at which this oxidation occurred ( $E_{\text{ox}}$ ). In Figure 1d, we showed already the average frequency of the peak for the many-molecules case, a behavior that resembled a linear shift as a function of the applied potential. Yet the result of Figure 1c,d is, to some degree, obscure in the sense that it includes in the signal the collective response of all molecules. The SM data displayed in Figure 5 provide the correct perspective for the interpretation of the observed potential dependence of the many-molecule Raman line shape and average peak position. Imagine we start with all of the

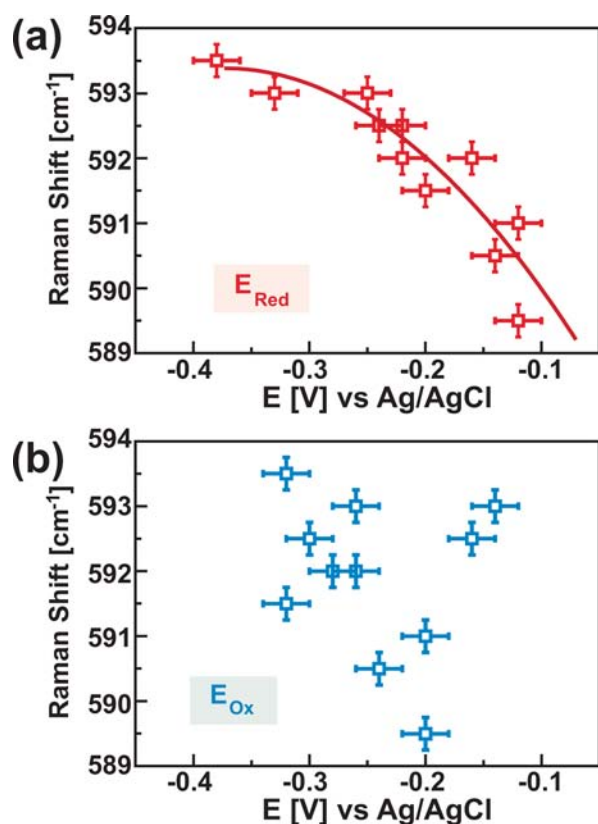


**Figure 5.** Dependence of the Raman shifts with the potential at which single NB oxidation (bottom) and reduction (top) events occur. Each point represents a single-molecule event.

molecules in the oxidized “on” state, and we start to sweep the potential toward reduction. Different molecules will be turning “off” at different stages of the cycle, and some will remain “on” while the potential is swept (until they reach their reduction potential). Because there is a correlation between the frequency of the mode and the reduction potential (resolved in Figure 5 for single-molecule cases), there will be a bias in the average frequency produced by the molecules that are already “off”, and those that remain “on” during the sweep. That is why the slope of the average signal is actually “smaller” than the slopes

observed in SM-SERS events versus potential. It is also quite clear from Figure 5 that oxidation and reduction follow completely different behavior. The explanation for this asymmetry is apparent: if the configurational changes of the molecules occur during the exchange of protons from/to the solution and electrons from/to the substrate (the signal “jumps” in Figures 3 and 4), it is natural to conclude that the Raman shift should correlate with the reduction potential produced after the “on”-state, and not with the oxidation process occurring before that state. In fact, the later should correlate with the vibrational frequencies of the “Raman silent” reduced state of the molecule. There is still the possibility that the changes occur not at the jumps, but before that during the silent (reduced) state that we cannot monitor with Raman.

The experimental facts are very clear; what remains is an interpretation of them. We speculate in what follows on several points that are revealed by this new type of experiments.

- Simplified models for the interactions of vibrations in molecules with surfaces are available in the literature, but present several limitations.<sup>31,32</sup> They are, for example, very sensitive to the actual choice of parameters. Nevertheless, within these limitations, it is possible to establish that a softening of a frequency (less energetic vibration) normally implies a slightly larger interaction with the surface. This would happen, for example, if the main effect of the metal substrate is to provide a dephasing channel for the molecular vibrations (as observed for temperature-dependent high-resolution SM-SERS experiments in ref 36). This is a manifestation of a very basic feature of a damped oscillator, that is, the softening of the resonance frequency when the damping is increased.
- Our experimental results evidence that molecules with a “weaker” interaction with the surface (i.e., harder frequencies, more energetic vibration) are reduced at much more negative potentials than molecules with a stronger interaction. From the different scenarios that might explain the existence of a collection of Raman shifts and electrochemical potentials in a molecular ensemble (subtle structural alterations of the molecules, effects of the solvent, molecule–surface distance, etc.), the latter provides a quite natural and closed explanation

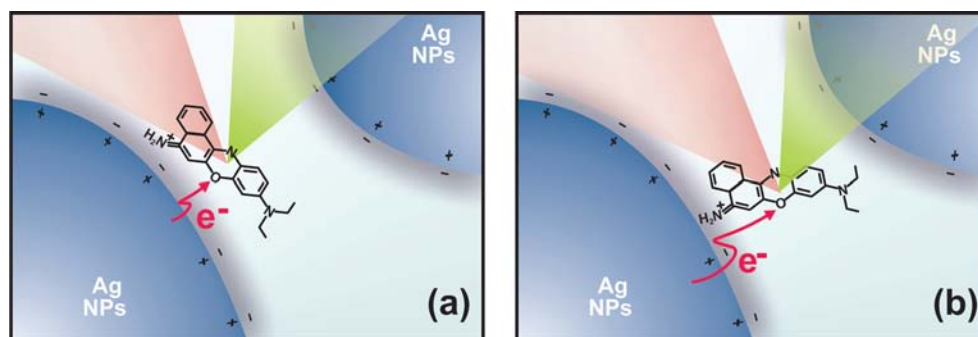


**Figure 6.** Scheme of the Ag NPs hot-spot/NB interface. The Ag surface has a potential of zero charge (PZC) of  $\sim -0.9$  V under similar experimental conditions. So, in the whole potential region scanned in our experiments, the surface is positively charged. An anionic layer (gray region) surrounds the NP surface, and NB molecules (cationic species in solution) interact electrostatically with them. Electron tunneling occurs through the anionic layer. Two possible situations where the molecule is located at different distances from the surface are shown. In (a) the shorter distance for the electronic tunneling facilitates charge transfer and a less negative reduction potential as compared to the situation depicted in (b). Considering a simplified model of an oscillator coupled to a dephasing channel (the substrate),<sup>31</sup> a shift toward lower frequencies is predicted for the Raman frequency when the molecule approaches to the surface.

for the main SM-electrochemistry-SERS experimental observations. In fact, molecules located closer to the metal surface would transfer electrons at a less negative potential than those located at higher distances according to the tunneling mechanism, and at the same time display higher vibrational dephasing rates (and thus smaller oscillation frequencies).

- Within our time resolution of  $\sim 100$  ms, we believe there is evidence for a specific charge-transfer mechanism between molecule and surface. The charge-transfer process that defines the oxidation/reduction happens in two units of charge in one direction and comes back to the original state upon reduction. The potentials at which these two events happen vary from molecule to molecule, and depend on the particular interaction of that molecule with the surface. The experimental results are compatible with molecules being “fixed” in the oxidized configuration (as revealed by the constancy of the frequency during that time), and presumably also in the reduced (Raman-silent) configuration, helped by the electrostatic interaction between both species and the surface.<sup>25</sup> Conversely, the fluctuating Raman shifts and their lack of correlation with the oxidation potential point toward a scenario in which the changes of molecule–substrate distance occur at the electron “jumps” associated with the oxidation/reduction of the molecule. These “jumps” are accompanied by the configurational changes associated with the addition of the two protons of the redox reaction. Another possibility is that the changes of molecule–substrate distance occur before in the silent (reduced) Raman state.

#### IV. CONCLUSIONS

It is possible to depict a “graphic summary” of the main findings in this Article, as shown in Figure 6, where two possible configurations of the molecule on the surface are considered. Accounting for the predictions of simplified oscillator models for the interaction of molecules with surfaces,<sup>30–32</sup> we observe that shorter distances favor charge transfer and vibration damping, and consequently a less negative reduction potential and smaller Raman frequencies. The two situations are compared in the figure. Single-molecule electrochemical experiments reveal in this case the subtle connection between the interaction with the surface (as revealed by a change in frequency) and the electrochemical properties of the cycle. The scope for more realistic calculations (beyond oscillator models) with Density Functional Theory (DFT) is opened from here, with the experimental motivation at hand. This phenomenology of the electrochemistry of single molecules can only be revealed by the simultaneous combination of (i) higher time resolution and (ii) higher spectral (frequency) resolution than previously used, and (iii) the use of reliable methods to identify single molecules (like the bianalyte technique). The combination opens a new door into electrochemical processes at the single-molecule level, and further extensions to other cases are easily envisioned.

#### ■ AUTHOR INFORMATION

##### Corresponding Author

emilianocll@gmail.com; afains@cab.cnea.gov.ar

##### Notes

The authors declare no competing financial interest.

#### ■ ACKNOWLEDGMENTS

E.C. would like to acknowledge the financial support of UNLP, ANPCyT (Argentina) and the MacDiarmid Institute (New Zealand) for a research/exchange program between Argentina and New Zealand. Thanks are also given to the host institution, Victoria University of Wellington, where the work was carried out. E.C., A.F., and R.C.S. are also at CONICET. M.E.V. is a member of the research career of CIC BsAs. P.G.E. and E.C.L.R. are indebted to the Royal Society of New Zealand for additional financial support under a Marsden Grant, and a Rutherford Discovery Fellowship.

#### ■ REFERENCES

- (1) Lei, C.; Hu, D.; Ackerman, E. J. *Chem. Commun.* **2008**, 5490.
- (2) dos Santos, D. P.; Andrade, G. F. S.; Temperini, M. L. A.; Brolo, A. G. *J. Phys. Chem. C* **2009**, *113*, 17737.
- (3) Xu, W.; Shen, H.; Kim, Y. J.; Zhou, X.; Liu, G.; Park, J.; Chen, P. *Nano Lett.* **2009**, *9*, 3968.
- (4) Ward, D. R.; Halas, N. J.; Ciszek, J. W.; Tour, J. M.; Wu, Y.; Nordlander, P.; Natelson, D. *Nano Lett.* **2008**, *8*, 919.
- (5) Moth-Poulsen, K.; Bjørnholm, T. *Nat. Nano* **2009**, *4*, 551.
- (6) Liu, Z.; Ding, S.-Y.; Chen, Z.-B.; Wang, X.; Tian, J.-H.; Anema, J. R.; Zhou, X.-S.; Wu, D.-Y.; Mao, B.-W.; Xu, X.; Ren, B.; Tian, Z.-Q. *Nat. Commun.* **2011**, *2*, 6.
- (7) Palacios, R. E.; Fan, F.-R. F.; Grey, J. K.; Suk, J.; Bard, A. J.; Barbara, P. F. *Nat. Mater.* **2007**, *6*, 680.
- (8) Hoeben, F. J. M.; Meijer, F. S.; Dekker, C.; Albracht, S. P. J.; Heering, H. A.; Lemay, S. G. *ACS Nano* **2008**, *2*, 2497.
- (9) Bard, A. J. *ACS Nano* **2008**, *2*, 2437.
- (10) Zhang, J.; Chi, Q.; Albrecht, T.; Kuznetsov, A. M.; Grubb, M.; Hansen, A. G.; Wackerbarth, H.; Welinder, A. C.; Ulstrup, J. *Electrochim. Acta* **2005**, *50*, 3143.
- (11) Kuznetsov, A. M.; Medvedev, I. G.; Ulstrup, J. *Electrochem. Commun.* **2009**, *11*, 1170.
- (12) Cortés, E.; Etchegoin, P. G.; Le Ru, E. C.; Fainstein, A.; Vela, M. E.; Salvezza, R. C. *J. Am. Chem. Soc.* **2010**, *132*, 18034.
- (13) Le Ru, E. C.; Etchegoin, P. G. *Principles of Surface Enhanced Raman Spectroscopy and Related Plasmonic Effects*; Elsevier: Amsterdam, **2009**.
- (14) Aroca, R. F. *Surface-Enhanced Vibrational Spectroscopy*; John Wiley & Sons: Chichester, **2006**.
- (15) Etchegoin, P. G.; Le Ru, E. C. *Anal. Chem.* **2010**, *82*, 2888.
- (16) Etchegoin, P. G.; Le Ru, E. C. *Phys. Chem. Chem. Phys.* **2008**, *10*, 6079.
- (17) Le Ru, E. C.; Meyer, M.; Etchegoin, P. G. *J. Phys. Chem. B* **2006**, *110*, 1944.
- (18) Goulet, P. J. G.; Aroca, R. F. *Anal. Chem.* **2007**, *79*, 2728.
- (19) Pieczonka, N. P. W.; Aroca, R. F. *Chem. Soc. Rev.* **2008**, *37*, 946.
- (20) Dieringer, J. A.; L., R. B., II; Scheidt, K. A.; Van Duyne, R. P. *J. Am. Chem. Soc.* **2007**, *129*, 16249.
- (21) Blackie, E. J.; Le Ru, E. C.; Etchegoin, P. G. *J. Am. Chem. Soc.* **2009**, *131*, 14466.
- (22) Etchegoin, P. G.; Le Ru, E. C.; Meyer, M. *J. Am. Chem. Soc.* **2009**, *131*, 2713.
- (23) Titus, E. J.; Weber, M. L.; Stranahan, S. M.; Willets, K. A. *Nano Lett.* **2012**, *12*, 5103.
- (24) Le Ru, E. C.; Etchegoin, P. G. *Annu. Rev. Phys. Chem.* **2012**, *63*, 65.
- (25) Ni, F.; Feng, H.; Gorton, L.; Cotton, T. M. *Langmuir* **1990**, *6*, 66.
- (26) Cortés, E.; Etchegoin, P. G.; Le Ru, E. C.; Fainstein, A.; Vela, M. E.; Salvezza, R. C. *Anal. Chem.* **2010**, *82*, 6919.
- (27) Creighton, J. A.; Blatchford, C. G.; Creighton, M. G. *J. Chem. Soc., Faraday Trans.* **1979**, *2*, 790.
- (28) Meyer, M.; Le Ru, E. C.; Etchegoin, P. G. *J. Phys. Chem. B* **2006**, *110*, 6040.

- (29) Zhang, P.; Cai, J.; Chen, Y.-X.; Tang, Z.-Q.; Chen, D.; Yang, J.; Wu, D.-Y.; Ren, B.; Tian, Z.-Q. *J. Phys. Chem. C* **2010**, *114*, 403.
- (30) Ford, G.; Weber, W. H. *Phys. Rep.* **1984**, *113*, 195.
- (31) Ford, G.; Weber, W. H. *Surf. Sci.* **1983**, *129*, 123.
- (32) Ueba, H. *J. Chem. Phys.* **1982**, *77*, 3759.
- (33) Lombardi, J. R.; Birke, R. L.; Lu, T.; Xu, J. *J. Chem. Phys.* **1986**, *84*, 4174.
- (34) Willets, K. A.; Stranahan, S. M.; Weber, M. L. *J. Phys. Chem. Lett.* **2012**, *3*, 1286.
- (35) Wang, Y.; Sevinc, P. C.; He, Y.; Lu, H. P. *J. Am. Chem. Soc.* **2011**, *133*, 6989.
- (36) Artur, C.; Le Ru, E. C.; Etchegoin, P. G. *J. Phys. Chem. Lett.* **2011**, *2*, 3002.